

Figure 6 Involvement of neurotrophins in the ProTx-induced retinal protection against ischemic damage. (a and b) Enhanced expression of various neurotrophic factors after retinal ischemic stress with or without ProTx. rmProTx α (100 μ g/kg, i.v.) was administered 3 h after retinal ischemic stress. Immunostaining of retinas was carried out at 24 h after ischemia–reperfusion (a). Western blot analysis of BDNF and EPO in retinas at 24 h after ischemia–reperfusion (b). Results represent the means \pm S.E.M. of four independent experiments. (c) rmProTx α (100 μ g/kg i.v.)-induced suppression of retinal ischemia-induced necrosis (PI staining) and apoptosis (TUNEL staining), and selective reversal of apoptosis by polyclonal anti-BDNF or polyclonal anti-EPO IgG. Anti-BDNF or anti-EPO IgG (1 μ g per eye) was i.v. injected at 30 min before the ischemic stress. (d) Fluorescence intensities were analyzed using NIH ImageJ software. Results represent the means \pm S.E.M. of 4–6 independent experiments. * P < 0.05 versus sham. † P < 0.05 versus ischemia vehicle treatment. ‡ P < 0.05 versus ischemia rmProTx α treatment

treatments with corresponding missense oligodeoxynucleotides (MS-ODNs) had no effect.

In vivo neuroprotective role of ProTx during retinal ischemia. As early as day 4 after ischemic stress, partial

damage to retinal cells was observed in the GCL, INL, and ONL (Figure 7a and Table 2). I.v.b pretreatment with an AS-ODN against ProTx, but not with a mismatch scrambled MS-ODN, significantly worsened the damage at day 4 after ischemic stress. Similar results were also observed following

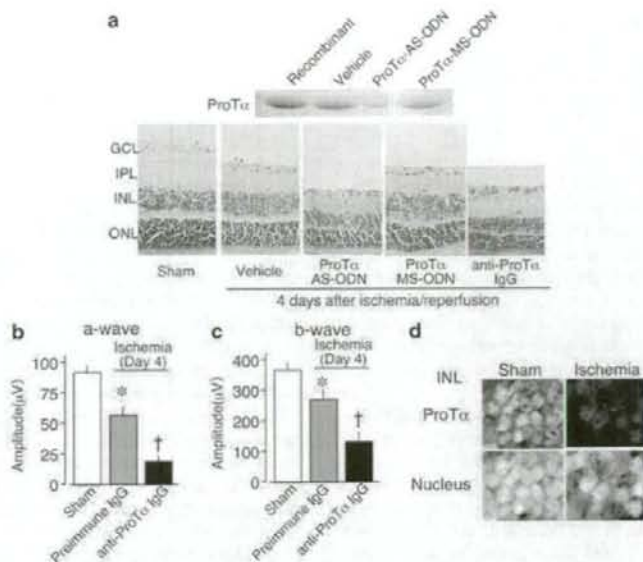


Figure 7 *In vivo* neuroprotective role of ProT α during retinal ischemia. (a) Worsening of retinal ischemic damage following treatment with anti-ProT α IgG (1 μ g per eye 30 min before ischemic stress) or an AS-ODN for ProT α . Retinas were isolated at day 4 after ischemic stress and used for histological studies. Upper panel: loss of ProT α protein in a retina pretreated with the AS-ODN, as evaluated by Gelatin Blue staining analysis.¹⁰ (b and c) Functional worsening of the retinal ischemic damage following treatment with anti-ProT α IgG or an AS-ODN for ProT α evaluated on the basis of a- (b) and b- (c) wave ERG analysis. The results represent the means \pm S.E.M. of six independent experiments. * $P < 0.05$ versus sham. † $P < 0.05$ versus ischemia vehicle treatment. (d) Depletion of immunoreactive ProT α in the INL of the retina at 3 h after ischemia–reperfusion

Table 2 *In vivo* neuroprotective role of ProT α during retinal ischemia

Treatment	Days after ischemia/reperfusion	GCL	INL	ONL
Sham+vehicle	4	16.53 \pm 1.23	128.71 \pm 5.93	299.61 \pm 28.69
Ischemia+vehicle	4	13.02 \pm 0.74	111.54 \pm 2.96	253.41 \pm 7.97*
Ischemia+ProT α AS-ODN	4	9.62 \pm 0.08 [#]	90.71 \pm 4.15 [#]	164.15 \pm 3.19 [#]
Ischemia+ProT α MS-ODN	4	13.62 \pm 0.58	110.91 \pm 5.34	266.10 \pm 7.97
Ischemia+ProT α IgG	4	10.51 \pm 1.07 [#]	94.30 \pm 8.30 [#]	221.54 \pm 15.94 [#]

Abbreviations: AS-ODN, antisense oligodeoxynucleotide; GCL, ganglion cell layer; IgG, immunoglobulin G; INL, inner nuclear layer; MS-ODN, missense oligodeoxynucleotide; ONL, outer nuclear layer

* $P < 0.05$ versus sham; [#] $P < 0.05$ versus ischemia vehicle treatment

i.vb pretreatment (1 μ g/eye, 30 min before ischemic stress) with anti-ProT α IgG, which absorbs ProT α ,¹⁰ which is released upon ischemic stress. In the ERG analysis, moreover, a weak but significant reduction in stimulation-induced a- and b-wave responses was observed at day 4 after the stress (Figure 7b and c). Anti-ProT α IgG injection further worsened the ischemia-induced functional damage. Moreover, the ProT α -like immunoreactivities, which were observed in the nuclei of INL cells in the sham-operated retinas, completely disappeared without exception 3 h after the stress (Figure 7d).

Discussion

Prothymosin- α , which is a highly acidic nuclear protein, is widely distributed throughout the body and is reported to play essential roles in the regulation of cell proliferation, as seen in

the facts that ProT α upregulates c-Myc and selectively enhances estrogen receptor transcriptional activity by interacting with a repressor of estrogen receptor activity.^{17–22} Furthermore, ProT α interacts with histones and affects chromatin remodeling processes through histone acetyltransferases to promote and stabilize the interaction of ProT α with the oncoprotein SET/TAF-1 β .^{23–25} Moreover, ProT α plays a cytoprotective role by inhibiting apoptosome formation in NIH3T3 cells subjected to apoptotic stress.²⁶ Moreover, a recent report demonstrated that ProT α liberates Nrf2 from a Keap1-Nrf2 inhibitory complex under oxidative stress and contributes to Nrf2-dependent gene expression.²⁷ In this mechanism, the transcription factor Nrf2 induces glutathione S-transferase, NAD(P)H-quinone oxidoreductase (NQO1), γ -glutamylcysteine synthetase and heme oxygenase-1.

We recently reported that ProT α , but not thymosin- α , inhibits the necrosis of cortical neurons treated with ischemic

or starvation stress.¹⁰ Under the condition of starvation stress, we found that membrane glucose transporters, such as GLUT1 and GLUT4, are internalized, thereby decreasing glucose transport in plasma membrane, leading to a rapid decrease in the intracellular adenosinetriphosphate (ATP) level. It should be noted that ProTx causes the apoptosis of cortical neurons in cultures subjected to starvation stress. As the addition of pyruvate, which inhibits necrosis by elevating cellular ATP levels, does not cause apoptosis in the same system, it is evident that ProTx-induced necrosis-inhibition and apoptosis-induction can be attributed to independent mechanisms.²⁸ However, this switch in cell death mode seems to have an important role in the protection of the brain in the event of stroke, as brain has potent anti-apoptosis systems, such as neurotrophins.¹¹ Indeed, we have demonstrated that the concomitant addition of neurotrophins with ProTx completely inhibited neuronal death, at least for 3 days, in an *in vitro* culture system.¹⁰

The present study provides *in vivo* evidence for the ProTx-induced switch in cell death mode. The first finding is that i.v.b or systemic administration of ProTx completely blocked retinal damage at day 7 after ischemia. This prevention of cell death was observed throughout the retina, including in neural fibers (IPL and OPL) as well as in the GCL, INL and ONL, when ProTx was administered 30 min before, or at 3 and 24 h after ischemia. As ERG study also showed that retinal function was protected, it appears that ProTx has potential for use protecting against retinal damage. It is known that material transport into the retina from the blood is limited by the blood-retina barrier, as in the case of the blood-brain barrier. In the present study, systemic administration of biotinylated rmProTx was detected in the retina, with ischemia. This finding is consistent with the report that systemic administration (i.v.) of EPO (MW: 18,519), which has a greater MW than ProTx (MW: 12,251), protects retinal neurons from ischemic damage.²⁹ We have also reported the ischemia-dependent transport of Myc-tagged ProTx to the brain 30 min after systemic administration (i.v.).¹¹ Thus, these findings suggest that damage to retinal capillary vessels by ischemic treatment allows the material to be freely transported.

The second finding is that necrosis occurs first and apoptosis later. In the present study, we used PI staining as a necrosis marker, although caspase-3 and TUNEL staining were used as apoptosis markers. The time course of necrosis and apoptosis incidents evaluated by TEM analysis clearly corresponded to that evaluated by PI staining and caspase-3 or TUNEL staining. We also found that there were no cortical neurons colabeled with PI-signal and caspase-3 (or TUNEL) signal following brain ischemia.¹¹ Thus, these markers seem to be valid for the characterization of cell death modes. Our initial speculation was that cell death initiated by necrosis in the core expands because of the subsequent release of cytotoxic molecules causing more necrosis. However, this cell death expansion was terminated by the occurrence of apoptosis, in which microglia removed damaged cells without releasing cytotoxic molecules. Although systemic administration of ProTx thoroughly abolished both necrosis and apoptosis after retinal ischemia, the concomitant application of anti-BDNF or anti-EPO IgG with ProTx or pretreatment of BDNF or EPO AS-ODN with ProTx caused marked apoptosis

as early as day 1 after the stress. However, these treatments alone had no effect on ischemia-induced cell death. As ProTx upregulated BDNF- and EPO-like immunoreactivities in the presence of ischemia, but not in its absence, ProTx-induced apoptosis must have been inhibited at the same time by the upregulated neurotrophins. From these findings, it is evident that a ProTx-induced switch in cell death mode occurs at day 1, but the machineries that underlie the delayed apoptosis at day 3 and its inhibition by ProTx remain to be elucidated. There are reports showing that many other cytotoxic molecules, such as cytokines and NO, cause delayed apoptosis.^{30,31} As the administered ProTx is unlikely to remain in the retina for 3 days, inhibition of delayed apoptosis by ProTx may be secondary to the initial prevention of rapid cell death, which may delay apoptosis through the production of cytotoxic molecules. Alternatively, the upregulation of neurotrophins by synergistic mechanisms induced by ProTx and ischemia may last for longer periods.

The major issue we addressed was whether or not ProTx has a neuroprotective role in ischemic retina. The present study successfully demonstrated that treatments with an AS-ODN against ProTx or anti-ProTx IgG worsened or accelerated retinal damage as detected by histochemistry and measurement of ERG functions. As ProTx was depleted from retinal cells upon ischemic stress, it is evident that released, not intracellular ProTx may afford retinal protection.

In conclusion, we demonstrated that ProTx inhibits necrosis of retinal cells, but causes apoptosis, which in turn is inhibited by endogenous and ProTx-induced neurotrophins. Along with this gain-of-function study, we also modeled loss of function of ProTx by using an AS-ODN and anti-ProTx IgG. We found that ProTx appears to have therapeutic potential for treatment of acute retinal ischemia, as the therapeutic window of systemic ProTx was later than 3 h after ischemic stress.

Materials and Methods

Preparation of recombinant proteins. Recombinant ProTx gene was amplified from cDNAs derived from mouse embryonic brains using specific primers: mouse 5' primer, 5'-AACATATGTCAGACGCGGAGTGA-3'; 3'-primer, 5'-GGATCCAAGCTGTGCTGTAGTATCCTGG-3'. The PCR products were cloned into pGEM-T Easy, and then subcloned into pET16b. BL21 (DE3) cells were transformed with pET16b-ProTx. Recombinant mouse ProTx were induced by 0.1 mM isopropylthio- β -galactopyranoside, purified by acid phenol extraction³² and Biophoresis (ATTO, Tokyo, Japan) separation, and dialyzed against phosphate-buffered saline (PBS) for later use. The purified recombinant proteins were used in experiments involving mouse retina preparations.

Animals and induction of ischemia-reperfusion injury. Male ddY mice were purchased from Tagawa Experimental Animals (Nagasaki, Japan), and subjected to a modified method for retinal ischemia-reperfusion injury. Briefly, ddY mice (30–40 g) were anesthetized with an intraperitoneal injection of sodium pentobarbital (75 mg/kg), and their pupils were fully dilated with 1% atropine sulfate drops. The anterior chamber was cannulated with a 33-gauge needle connected to a container of sterile intraocular irrigating solution (BSS PLUS dilution buffer; Alcon, Fort Worth, TX, USA). Retinal ischemia was induced by elevating the IOP to generate a hydrostatic pressure of 130 mm Hg for 45 min by lifting the container. The retina was isolated at the indicated time points after ischemia-reperfusion treatment and the extent of damage was evaluated by hematoxylin and eosin staining. The numbers of cells for these measurements, taken in five adjacent areas (one area: 100 μ m) within 1 mm of the optic nerve, were calculated (Tables 1 and 2). Data are the means \pm S.E.M. from 4 to 6 independent experiments. ProTx AS-ODN (5'-ATCGCCGGTCTGACATGGT-3'), MS-ODN (5'-AGTCAGCTTCGCACCTG GT-3'), BDNF AS-ODN (5'-CATCACTTCTCACTGGTGAAC-3'), MS-ODN

(5'-GTTCCACCCAGGTGAGAAGAGTGATG-3')²³ EPO AS-ODN (5'-CTCACCCG GCACCCCAT-3') and MS-ODN (5'-ATGGGGTGGCCGGTGGAG-3')²⁴ were i.v. injected (1 nmol per eye) at 5, 3 or 1 day before ischemic stress. Anti-BDNF or anti-EPO antibody (Santa Cruz Biotechnology, Tokyo, Japan) were i.v. injected at 30 min before ischemic stress. Animal care and experimental procedures were performed in accordance with conformed to the Guidelines for Animal Experimentation of Nagasaki University with the approval of the Institutional Animal Care and Use Committee.

Electroretinogram. The mice were tested after 3 h of dark adaptation. They were anesthetized with intraperitoneal pentobarbital sodium. Their pupils were dilated with 1% atropine. A contact electrode (KE-S; Kyoto contact lenses, Kyoto, Japan) was placed on the corneal apex and referenced to a needle electrode near the eye. The ground was a subdermal platinum needle electrode near the abdominal area. ERGs were produced by 20J flash intensities. The flash stimulus source (SLS-3100; Nihon Kohden, Tokyo, Japan) illuminated the eye by diffuse reflection off the interior surface of the Ganzfeld. Maximum flash luminance was measured with detector (MEB-9104; Nihon Kohden, Tokyo, Japan). After the intensity series, an incandescent background light sufficient to desensitize the rod system was turned on, and ERGs produced by the standard stimulus were recorded every 2 min for 20 min. The background was then turned off, and ERGs were produced by the standard stimulus every 2 min for the first 30 min of dark adaptation. The a- and b-wave amplitudes were measured online (Neuropack m; QP-903B, Nihon Kohden, Tokyo, Japan).

Transmission electron microscopy. Retinas treated with ischemia-reperfusion were fixed with 2.5% glutaraldehyde in 0.1 M phosphate buffer (pH 7.4) for 1 h at 25°C, postfixed with 1% osmium tetroxide for 1 h at 25°C, dehydrated through a graded alcohol series and embedded in Epon812 resin. Ultrathin sections (80-nm thick) were cut with an Ultracut S (Leica, Vienna, Austria), and then stained with uranyl acetate and lead citrate for 30 and 5 min, respectively. The stained sections were observed under an electron microscope (JEM-1210; JEOL, Tokyo, Japan). TEM analysis was used to characterize the cell death mode in the retinas at 24 h after the ischemia-reperfusion treatment. The numbers of necrotic and apoptotic cells for these measurements, taken in 30–50 adjacent areas (one area: 8 × 12 μm) within 3 mm of the optic nerve, were calculated (Figures 2 and 3).

In vivo retinal PI staining. For PI (Sigma, Tokyo Japan) staining experiments, mice were anesthetized with sodium pentobarbital and i.v. injected with PI (2 ng per eye) 1 h before collection of their retinas. The retinas were removed, fixed in 4% paraformaldehyde (PFA) in K⁺-free PBS and cryoprotected overnight in 25% sucrose in K⁺-free PBS. Retinas were fast-frozen in a cryoembedding compound on a mixture of ethanol and dry ice and stored at -80°C until use. The retinas were cut into 10-μm sections using a cryostat, thaw-mounted onto silane-coated glass slides and examined under a fluorescence microscope (Olympus, Tokyo, Japan). The fluorescence intensities of the PI-signals were quantified using NIH Image for Macintosh. The counting region of PI fluorescence intensities was from the GCL to the ONL, but not the EPI region because, in the EPI, PI signal was observed throughout the sham-operated retina, which is liable to be damaged and artificially stained with PI during the process of sample preparation.

Apoptosis staining of retinal sections. Retinal sections (10 μm) were rinsed twice with PBS and reacted with TUNEL (Invitrogen, Tokyo Japan) solution from Roche Molecular Biochemicals for 1 h at 37°C. They were washed twice in PBS and added to blocking buffer (1% bovine serum albumin (BSA) in PBS, pH 7.4) for 1 h at 25°C, followed by incubation with streptavidin-fluorescein isothiocyanate (1:100; Vector Laboratories, Burlingame, CA, USA) for 1.5 h at 25°C. Immunolabeled sections were mounted with Permafluor (Thermo Shandon, Pittsburgh, PA, USA), and examined under a fluorescence microscope (Olympus, Tokyo, Japan). Moreover, for active caspase-3 immunostaining, retinal sections (10 μm) were rinsed twice with PBS and preincubated in blocking buffer (3% BSA and 0.1% Tween 20 in PBS) for 1 h at 25°C. Next, the sections were incubated with polyclonal anti-active caspase-3 (1:100 dilution in blocking buffer; Cell Signaling, Tokyo, Japan) overnight at 4°C, rinsed with PBS and incubated with Alexa 488-conjugated anti-rabbit IgG (1:200 dilution; Invitrogen) for 2 h at 25°C. Other sections were fixed with 4% PFA in PBS for 30 min, and permeabilized with 50 and 100% methanol for 5 min each. Immunolabeled sections were mounted with Permafluor, and examined under a fluorescence microscope. The fluorescence

intensities of the caspase-3 signals were quantified using NIH ImageJ software for Macintosh.

Western blot analysis. SDS-polyacrylamide gel electrophoresis using 10–12% polyacrylamide gels and immunoblot analysis was performed as described previously.²⁵ Anti-BDNF, anti-EPO, anti-nerve growth factor and anti-bFGF IgG (1:500; Santa Cruz Biotechnology) were used as the primary antibodies. Visualization of immunoreactive bands was performed using an enhanced chemiluminescent substrate (Super Signaling Substrate; Pierce Chemical Co., Rockford, IL, USA) for the detection of horseradish peroxidase. The specificity of polyclonal anti-BDNF and anti-EPO antibodies is described in the Supplementary text and Supplementary Figure 4.

Statistical analysis. For statistical analysis of the data, Student's *t*-tests following multiple comparisons by analysis of variance were used. The criterion of significance was set at *P* < 0.05. All results are expressed as means ± S.E.M.

Acknowledgements. This study was supported by Grants-in-Aid for Scientific Research (to HU, B: 13470490 and 15390028), on Priority Areas – Research on Pathomechanisms of Brain Disorders (to HU, 17025031, 18023028, 20023022) from the Ministry of Education, Culture, Sports, Science and Technology (MEXT) and Encouragement of Young Scientists (to RF, B: 17790066 and 19790191) from the Japan Society for the Promotion of Science (JSPS). Also, Health and Labour Sciences Research Grants on Research on Biological Resources and Animal Models for Drug Development from Ministry of Health, Labour and Welfare (to HU, H20-Research on Biological Resources and Animal Models for Drug Development-003). We gratefully acknowledge A Akaie for technical advice in the retinal ischemia study, M Niwa and T Suetatsu for technical assistance in the TEM studies and H Matsunaga, M Rikumar, Y Kiguchi (Tobo) and S Kawakami for technical assistance with the retinal ischemia.

- Dimagi U, Iadecola C, Moskowitz MA. Pathobiology of ischaemic stroke: an integrated view. *Trends Neurosci* 1999; **22**: 391–397.
- Lipton P. Ischemic cell death in brain neurons. *Physiol Rev* 1999; **79**: 1431–1568.
- Ueda H, Fujita R. Cell death mode switch from necrosis to apoptosis in brain. *Biol Pharm Bull* 2004; **27**: 950–955.
- Brines ML, Ghezzi P, Keenan S, Agnello D, de Lanerolle NC, Cerami C et al. Erythropoietin crosses the blood-brain barrier to protect against experimental brain injury. *Proc Natl Acad Sci USA* 2000; **97**: 10526–10531.
- Cheng Y, Deshmukh M, D'Costa A, Demaro JA, Gidday JM, Shah A et al. Caspase inhibitor affords neuroprotection with delayed administration in a rat model of neonatal hypoxic-ischemic brain injury. *J Clin Invest* 1998; **101**: 1992–1999.
- Gilgun-Sherki Y, Rosenbaum Z, Melamed E, Offen D. Antioxidant therapy in acute central nervous system injury: current state. *Pharmacol Rev* 2002; **54**: 271–284.
- Gladstone DJ, Black SE, Hakim AM. Toward wisdom from failure: lessons from neuroprotective stroke trials and new therapeutic directions. *Stroke* 2002; **33**: 2123–2136.
- Fujita R, Ueda H. Protein kinase C-mediated necrosis-apoptosis switch of cortical neurons by conditioned medium factors secreted under the serum-free stress. *Cell Death Differ* 2003; **10**: 782–790.
- Fujita R, Yoshida A, Mizuno K, Ueda H. Cell density-dependent death mode switch of cultured cortical neurons under serum-free starvation stress. *Cell Mol Neurobiol* 2001; **21**: 317–324.
- Ueda H, Fujita R, Yoshida A, Matsunaga H, Ueda M. Identification of prothymosin-α1, the necrosis-apoptosis switch molecule in cortical neuronal cultures. *J Cell Biol* 2007; **176**: 853–862.
- Fujita R, Ueda H. Prothymosin-α1 prevents necrosis and apoptosis following stroke. *Cell Death Differ* 2007; **14**: 1839–1842.
- Isemann S, Kretz A, Cellerino A. Molecular determinants of retinal ganglion cell development, survival, and regeneration. *Prog Retin Eye Res* 2003; **22**: 483–543.
- Choi DW. Ischemia-induced neuronal apoptosis. *Curr Opin Neurobiol* 1996; **6**: 667–672.
- Lombardi G, Moroni F, Moroni F. Glutamate receptor antagonists protect against ischemia-induced retinal damage. *Eur J Pharmacol* 1994; **271**: 489–495.
- Block F, Schwarz M. The b-wave of the electroretinogram as an index of retinal ischemia. *Gen Pharmacol* 1998; **30**: 281–287.
- Unal Cevik I, Dalkara T. Intravenously administered propidium iodide labels necrotic cells in the intact mouse brain after injury. *Cell Death Differ* 2003; **10**: 928–929.
- Clinton M, Graeve L, el-Domy H, Rodriguez-Boulan E, Horecker BL. Evidence for nuclear targeting of prothymosin and parathyroidin synthesized *in situ*. *Proc Natl Acad Sci USA* 1991; **88**: 6608–6612.
- Gaubatz S, Meichle A, Eilers M. An E-box element localized in the first intron mediates regulation of the prothymosin alpha gene by c-myc. *Mol Cell Biol* 1994; **14**: 3853–3862.

19. Letsas KP, Frangou-Lazaridis M. Surfing on prothymosin alpha proliferation and anti-apoptotic properties. *Neoplasia* 2006; **53**: 92–96.
20. Martini PG, Delage-Mouroux R, Kraichely DM, Katzenellenbogen BS. Prothymosin alpha selectively enhances estrogen receptor transcriptional activity by interacting with a repressor of estrogen receptor activity. *Mol Cell Biol* 2000; **20**: 6224–6232.
21. Pineiro A, Cordero OJ, Nogueira M. Fifteen years of prothymosin alpha: contradictory past and new horizons. *Peptides* 2000; **21**: 1433–1446.
22. Segade F, Gomez-Marquez J. Prothymosin alpha. *Int J Biochem Cell Biol* 1999; **31**: 1243–1248.
23. Gomez-Marquez J. Function of prothymosin alpha in chromatin decondensation and expression of thymosin beta-4 linked to angiogenesis and synaptic plasticity. *Ann NY Acad Sci* 2007; **1112**: 201–209.
24. Karetsov Z, Martic G, Tavoulari S, Christoforidis S, Wilm M, Gruss C et al. Prothymosin alpha associates with the oncoprotein SET and is involved in chromatin decondensation. *FEBS Lett* 2004; **577**: 496–500.
25. Karetsov Z, Sandaltzopoulos R, Frangou-Lazaridis M, Lai CY, Tsolas O, Becker PB et al. Prothymosin alpha modulates the interaction of histone H1 with chromatin. *Nucleic Acids Res* 1998; **26**: 3111–3118.
26. Jiang X, Kim HE, Shu H, Zhao Y, Zhang H, Kolron J et al. Distinctive roles of PHAP proteins and prothymosin-alpha in a death regulatory pathway. *Science* 2003; **299**: 223–226.
27. Karapetian RN, Evstafieva AG, Abaeva IS, Chichkova NV, Filonov GS, Rubtsov YP et al. Nuclear oncoprotein prothymosin alpha is a partner of Keap1: implications for expression of oxidative stress-protecting genes. *Mol Cell Biol* 2005; **25**: 1089–1099.
28. Fujita R, Ueda H. Protein kinase C-mediated cell death mode switch induced by high glucose. *Cell Death Differ* 2003; **10**: 1336–1347.
29. Junk AK, Mammis A, Savitz SI, Singh M, Roth S, Malhotra S et al. Erythropoietin administration protects retinal neurons from acute ischemia–reperfusion injury. *Proc Natl Acad Sci USA* 2002; **99**: 10659–10664.
30. Tezel G, Wax MB. Increased production of tumor necrosis factor-alpha by glial cells exposed to simulated ischemia or elevated hydrostatic pressure induces apoptosis in cocultured retinal ganglion cells. *J Neurosci* 2000; **20**: 8693–8700.
31. Toda N, Nakanishi-Toda M. Nitric oxide: ocular blood flow, glaucoma, and diabetic retinopathy. *Prog Retin Eye Res* 2007; **26**: 205–238.
32. Evstafieva AG, Chichkova NV, Makarova TN, Vartapetian AB, Vasilenko AV, Abramov VM et al. Overproduction in *Escherichia coli*, purification and properties of human prothymosin alpha. *Eur J Biochem* 1995; **231**: 639–643.
33. Mandolesi G, Menna E, Harauzov A, von Bartheld CS, Caleo M, Maffei L. A role for retinal brain-derived neurotrophic factor in ocular dominance plasticity. *Curr Biol* 2005; **15**: 2119–2124.
34. Liu J, Narasimhan P, Song YS, Nishi T, Yu F, Lee YS et al. Epo protects SOD2-deficient mouse astrocytes from damage by oxidative stress. *Glia* 2006; **53**: 360–365.

Supplementary Information accompanies the paper on Cell Death and Differentiation website (<http://www.nature.com/cdd>)